JOURNAL OF CATALYSIS **120**, 303–313 (1989)

Fourier Transform–Infrared Spectroscopic Study of the Adsorption of Hydrogen on Chromia and on Some Metal Chromites

GUIDO BUSCA

Istituto di Chimica, Facoltà di Ingegneria, Università di Genova, Piazzale Kennedy, 16129 Genoa, Italy

Received January 24, 1989; revised April 25, 1989

Adsorption of hydrogen and deuterium on samples of chromia and on nonstoichiometric zinc, cobalt, and manganese chromites (M/Cr atomic ratio 1 : 1; M = Zn, Co, Mn), previously activated in hydrogen and vacuum, was studied by means of Fourier transform–infrared spectroscopy. Parallel CO adsorption experiments indicate that all four catalysts are essentially in an oxide form after hydrogen adsorption. Only in the case of the cobalt compound are zerovalent centers observed. Terminal hydrides Cr–H are formed on chromia, whereas on the three chromites, both terminal and bridged hydride species, thought to be bonded to Zn^{2+}, Co^{2+}, and Mn^{2+} centers, respectively, are observed. These assignments are based on the H(D) isotopic shift and on a comparison with the spectra of known hydride species of the same metals. The mechanism of formation of these adsorbed forms is briefly discussed.

INTRODUCTION

Chromia is an active catalyst for hydrogenation reactions such as olefin hydrogenation (*1*, *2*), methanol synthesis (*3*, *4*), and hydrodealkylation of toluene (*5*) as well as for the water–gas shift equilibrium (*4*). The interaction of hydrogen with chromia has been the object of several studies (*1*, *2*, *6*, *7*). However, no direct spectroscopic evidence of the state of adsorbed hydrogen has been reported so far.

Metal chromites, such as copper (*8*), zinc (*9*), and manganese (*10*) chromites, have been largely used in industry as hydrogenation catalysts for fatty ester hydrogenation, methanol synthesis, and methanol–higher alcohol mixture synthesis, respectively (*11*), and are now the object of renewed interest. These "mixed oxide" catalysts can be regarded as nonstoichiometric chromites having a M/Cr atomic ratio ≥ 1 (M = Cu, Zn or Mn) and are believed to be more active and/or more stable than both chromia and the parent oxides of the element M, on the one hand, and the stoichiometric spinels MCr_2O_4 (M/Cr atomic ratio 0.5), on the other hand. Recently, also nonstoichiometric cobalt chromites have been reported to be active catalysts for CO hydrogenation (*12*).

Because of our interest in CO hydrogenation catalysts (*13*, *14*), we undertook a Fourier transform–infrared spectroscopic (FT-IR) study of hydrogen adsorption on α-chromia and on nonstoichiometric zinc, cobalt, and manganese chromites. The aim was to obtain data on the nature of adsorbed hydrogen species on these active catalysts, to understand better the role of different catalyst phases and the mechanisms of these reactions.

EXPERIMENTAL

Some data on the oxide catalysts used for the present study and references in which their preparation, characterization, and catalytic behavior are described in detail are reported in Table 1. All samples have been pressed into self-supporting disks (1 cm in diameter, 10–30 mg) and activated in the IR cell by evacuation (10^{-5} torr) at 790 K for 2 h, heating at 790 K in hydrogen (1 atm) for 1 h, and again evacuation at 790 K for 1 h. The samples were then cooled to room temperature and brought into contact with hydrogen and carbon monoxide (130 Torr) at room temperature. The IR spectra were re-

0021-9517/89 $3.00

TABLE 1

Characteristics of Oxide Catalysts Used in the Present Study

Notation	Composition	XRD Phases	Surface Area (m^2 g^{-1})	Preparation	Ref.
Chromia	Cr_2O_3	α-Cr_2O_3	44	Fumed[a]	—
ZnCr	Zn : Cr 1 : 1	Spinel	119	Coprec.[b]	(*15*)
CoCr	Co : Cr 1 : 1	Spinel	101	Coprec.	(*12, 16*)
MnCr	Mn : Cr 1 : 1	Spinel[c]	110	Coprec.	(*17*)

[a] From Degussa (Hanau, West Germany).
[b] Coprecipitated.
[c] Poorly crystalline.

corded with a Nicolet 5ZDX Fourier transform spectrometer (270 scans, 2 cm^{-1} resolution). The gas-phase spectrum was subtracted when necessary.

Hydrogen (purity > 99.5%) was taken from commercial cylinders supplied by SIO (Milano, Italy) and dried over P_2O_5 before use.

RESULTS

Investigation of Surface Oxidation State through CO Adsorption

To have an idea of the oxidation state of the oxide surfaces after the cited pretreatment, the spectra of the activated samples and of the species arising from CO adsorption have been previously examined. The absence of Cr═O stretching bands in the region near and below 1000 cm^{-1}, well evident on the calcined surfaces, indicates that Cr^{6+} species have been reduced upon pretreatment in all cases. The FT-IR spectrum in the skeletal region of the powder after this treatment is still that of α-Cr_2O_3. The spectra of the adsorbed species formed on the activated catalyst surfaces by contact with CO at 130 Torr and room temperature are reported in Figs. 1 and 2. On chromia a band is observed at 2180 cm^{-1}, with shoulders at 2188, 2173, and 2163 cm^{-1}. This result is essentially the same as that reported by Zecchina and co-workers on a similar polycrystalline sample (*18*). Recently, the same research group showed that the main band is due to interaction of CO with Cr^{3+} centers on the (0001) face of the hexagonal corundum-type α-chromia structure, with shifts toward lower frequencies on an increase in coverage, due to adsorbate–adsorbate interactions (*19*). A band at 2162 cm^{-1} was also found by these authors, but only at low temperature (77 K); it was assigned to a similar carbonyl

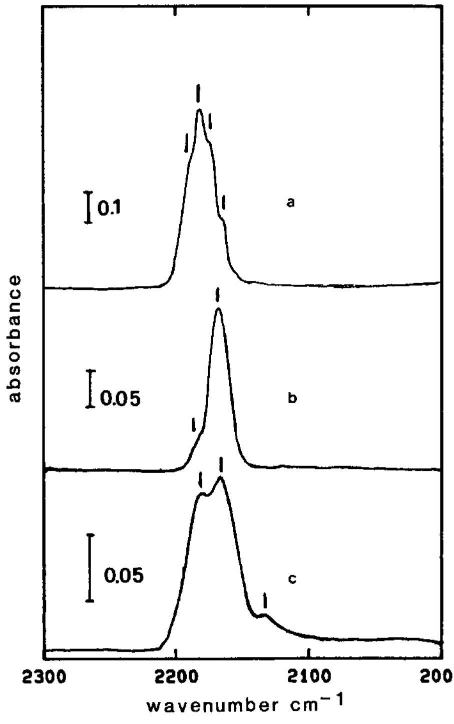

FIG. 1. FT-IR spectra of CO (120 Torr) adsorbed on activated chromia (a), ZnCr oxide (b), and MnCr oxide (c).

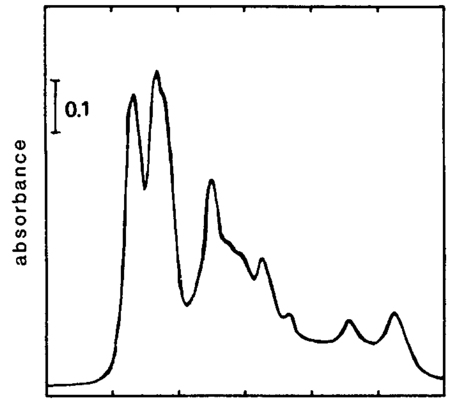

FIG. 2. FT-IR spectrum of CO (120 Torr) adsorbed on activated CoCr oxide.

species bonded on surface Cr^{3+} ions exposed on prismatic faces (*19*). In this last work, the reduction treatments were shorter than ours but at a higher temperature (973 K). As a result of the lower-temperature treatment and a certainly very different morphology, our sample very probably contains a greater exposure of prismatic faces and of surface defects than that of Scarano *et al.* (*19*). This explains the somewhat more complex spectrum we observe after CO adsorption at room temperature. In any case the absence of bands at frequencies lower than 2140 cm^{-1} would indicate that in both cases, no Cr species in a reduced state is present. Thus, the spectrum of adsorbed CO indicates that on the activated chromia suurface, Cr^{3+} ions are essentially exposed. These sites arise from the octahedrally coordinated cations typical of the α-Cr_2O_3 structure, but having one or two degrees of coordinative unsaturation, according to their location on the surface (*19*).

A band near 2170 cm^{-1} is observed when all three chromite samples are exposed to CO. This band is consequently assigned to CO on Cr^{3+} ions in an incomplete octahedral coordination in all cases. In the stoichiometric metal chromites, which are normal spinels (*20*), chromium(III) occupies the octahedral position because of its very high ligand field stabilization energy for octahedral coordination. With the ZnCr catalyst a shoulder is also evident, near 2190 cm^{-1} under these conditions, and could be due to CO on Zn^{2+} centers (*13*). With the MnCr catalyst a stronger maximum is observed at 2165 cm^{-1}, with another band near 2180 cm^{-1} and a weak shoulder near 2135 cm^{-1}. The bands at 2180 and 2135 cm^{-1} can be assigned to interacting CO with unreduced Mn centers, Mn^{3+} and/or Mn^{2+} (*21–23*). The absence of bands below 2100 cm^{-1} allows us to exclude the formation of manganese metal particles upon reductive pretreatment (*21*).

Detailed characterization of the state of the bulk has been carried out for both ZnCr (*9, 13*) and CoCr (*16*) oxides, and it is considered that after reduction both oxides are in the form of spinels which have evolved partially toward a rock salt-type structure, due to the excess of bivalent cations (Zn^{2+} and Co^{2+}, respectively) with respect to the spinel stoichiometry.

From CO adsorption we conclude that even after our reductive pretreatment, the chromia, ZnCr, and MnCr samples are all in an oxide state, without formation of metal species. A quite different picture is observed when CO is brought into contact with the CoCr catalyst (Fig. 2). In this case, together with the band at 2171 cm^{-1}, assigned to CO on Cr^{3+}, and two bands with a similar stability observed at 2137 and 2122 cm^{-1}, assigned to CO on incompletely reduced cobalt centers [most probably Co^{2+} and/or Co^{+} centers (*21, 23*)], several quite strong bands are observed in the region 2100–1700 cm^{-1}. The general picture is similar to that observed for supported cobalt polycarbonyls (*24*) and for partly reduced cobalt oxide on silica (*25*). In particular we note the presence of bands typical of bridged (1850 cm^{-1}) and triply bridged (1780 cm^{-1}) CO in cobalt carbonyl clusters. A detailed interpretation of the behavior of these bands upon pressure variations and evacuation treatments and their assignment will be reported elsewhere (*16*). What is relevant to the present study is that the complex spectra observed after CO adsorption indicate that reduced zerovalent Co centers probably in the form of very small clusters are present on the activated CoCr catalyst after CO adsorption. They may result from the reductive pretreatment or may be formed by interaction with CO. In fact, carbonate species are also formed as a result of CO oxidation. We cannot exclude then that zerovalent cobalt is involved in hydrogen adsorption on CoCr. However, massive cobalt metal particles do not seem to be present. In that case an evacuation-resistant band centered at 2050–1990 cm^{-1} should be observed (*21, 25, 26*).

TABLE 2

Summary of IR Bands due to Adsorbed Hydrogen

Catalyst	ν(MH)	ν(MD)	ν(MH)/ν(MD)	Assignment
Cr_2O_3	1714	1240	1.382	ν(Cr–H)
	1697	1229	1.381	ν(Cr–H)
ZnCr	1815	1315	1.380	ν(Zn–H)
	1788	1295	1.381	ν(Zn–H)
	1460	1065	1.371	ν_{as}(Zn–H–Zn)
MnCr	1506	1090	1.382	ν(Mn–H)
	1240	900	1.378	ν_{as}(Mn–H–Mn)
CoCr	1762	1276	1.381	ν(Co–H)
	1660	1200	1.383	ν(Co–H)
	1605	1160	1.383	ν_{as}(Co–H–Co)
	990			ν_s(Co–H–Co)
	875			δ(CoH)

Hydrogen Adsorption

Spectra of activated Cr_2O_3 and those recorded after hydrogen and deuterium adsorption are reported in Fig. 3. The spectrum of crystalline chromia shows, in the region below 1400 cm^{-1}, several absorptions due to overtones and combinations of the fundamental lattice vibrations (*27*). When hydrogen is brought into contact with the sample a weak but well-evident new band is formed, having a minor maximum at 1714 cm^{-1} and a main maximum at 1697 cm^{-1}. The region where this band falls strongly suggests assignment to a metal–hydrogen vibration. If the contact is carried out with deuterium this band is not detected, but another one grows superimposed on a lattice combination near 1235 cm^{-1} (*27*). The new band is seen more clearly by ratioed spectra, where the chromia background has been subtracted, and seems to consist of two absorptions not well resolved, near 1240 cm^{-1} and at 1229 cm^{-1}. The ratio between the absorption frequencies detected after hydrogen and deuterium adsorption is the correct one for M–H(D) stretches (see Table 2). The sharp band we observe, weakly split, lies in a region similar to that of the Cr–H stretches of terminal chromium hydride complexes (Table 3). The asymmetric metal–hydrogen–metal stretch of bridged hydride species can also fall at such a high frequency if the M–H–M angle is very high (*34*). However, the bands of bridged hydrides are broad at room temperature, in contrast to the one we observed which, although weak, is very sharp. The splitting could be due to the formation of two slightly different species. Adsorption of hydrogen and deuterium also causes the growth of bands in the ν(OH)

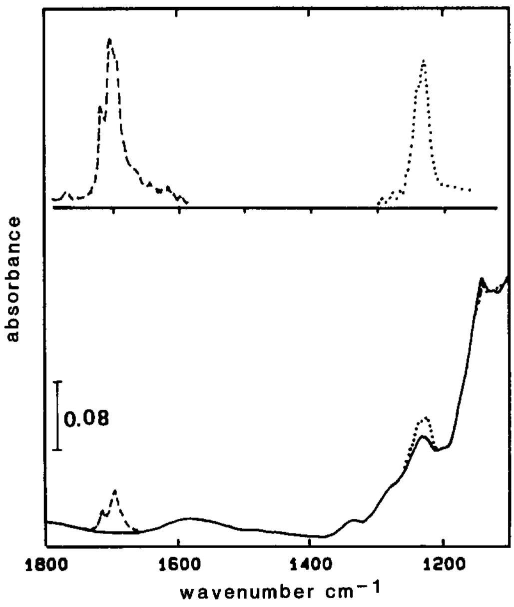

FIG. 3. FT-IR spectra of chromia after activation (solid line) and after contact with hydrogen (120 Torr; broken line) and deuterium (120 Torr; dotted line). In the inset the corresponding subtraction spectra are reported.

TABLE 3

ν(MH) Wavenumbers (cm^{-1}) for Selected Metal Hydride Compounds[a]

Complex	State	ν(MH)	ν(MD)	Hydride type	Ref.
CrH	Gas	1581		Terminal	(*30*)
	Matrix	1548		Terminal	(*30*)
CrH_2	Matrix	1591	1145	$\nu_{as}CrH_2$	(*30*)
$[CrH(CO)_3Cp]$		1765		Terminal	(*31*)
$[CrH(L)_2]BEt_4$		1895		Terminal	(*32*)
$[CrH_4(L')_2]$		1757 1725 1701		All terminal	(*33*)
$[Cr_2H(CO)_{10}]^-$		1720		$\nu_{as}CrHCr$	(*34*)
		818		ν_sCrHCr	
ZnH	Gas	1709		Terminal	(*35*)
$[ZnH(NMe_2C_2H_4NMe)]_2$		1825		Terminal	(*36*)
$HZnCH_3$	Matrix	1846		Terminal	(*37*)
HZnCH	Matrix	1924		Terminal	(*38*)
$[ZnH(C_6H_5)_2]Na$		1650–1250	1200–900	Bridged?	(*39*)
$[ZnH(CH_3)_2]Li$		1450	1041	Bridged?	(*40*)
$[CoH(P(OEt)_3)_4]$		1964		Terminal	(*41*)
$[CoH(CO)_4]$		1934		Terminal	(*42*)
$[CoH_2(PHPh_2)_4]$		1945, 1910		Terminal	(*43*)
$[CoH(CN)_5]^{3-}$		1840		Terminal	(*44*)
$HCoCH_3$		1699		Terminal	(*37*)
$[CoH(Cp)]_4$		(1050)		$\nu_s(Co)_3H$	
		958		$\nu_{as}(Co)_3H$	(*45*)
MnH	Gas	1491		Terminal	(*35*)
	Matrix	1479	1066	Terminal	(*46*)
MnH_2	Matrix	1594	1156	$\nu_{as}MnH_2$	(*46*)
$[MnH(PF_3)_5]$		1845		Terminal	(*47*)
$[HMn(CO)_5]$		1780		Terminal	(*48*)
$HMnCH_3$	Matrix	1583		Terminal	(*37*)
$Mn_3H_3(CO)_{12}$		1660, 1605	1245, 1162	$\nu_{as}MnHMn$	(*49*)
		900–824	700–650	ν_sMnHMn	
$Mn_3H(CO)_{10}$		1000		$\nu MnHMn$	(*50*)

[a] L = $(Me_2PCH_2)_3CMe$; L′ = $Me_2PC_2H_4PMe_2$; Cp = $[C_5H_5]^-$.

and ν(OD) regions, respectively, superimposed on those of "normal" hydroxy and deuteroxy groups residual from water and heavy water dissociation.

Adsorption of hydrogen on the ZnCr oxide causes the formation of a very strong band whose main maximum is observed near 1800 cm^{-1} but having a second component at 1815 cm^{-1} and a tail at lower frequencies. The main maximum of this band shifts upward with an increase in the activation temperature. Analogously, a corresponding band is observed upon deuterium adsorption (Fig. 4). The assignment of these bands to terminal zinc hydride and deuteride species has already been described (*28*).

Under these conditions, there appears another broader band whose main maximum is observed near 1460 cm^{-1} with a shoulder near 1390 cm^{-1}. A similarly shaped band is observed after contact with D_2 centered near 1065 cm^{-1}. This last band is superimposed on a sharp band that grows after both hydrogen and deuterium adsorption near 965 cm^{-1}, due to a variation of a

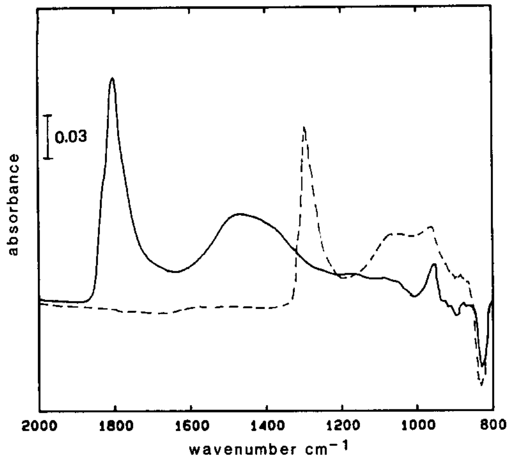

FIG. 4. FT-IR spectra of the adsorbed species arising from contact of activated ZnCr oxide with hydrogen (120 Torr; solid line) and deuterium (120 Torr; broken line).

surface species that does not involve hydrogen. Hence, the frequency of the shoulder cannot be determined after deuterium adsorption. The assignment of these bands to bridged zinc hydrides and deuterides is well substantiated by the similarity of the band with that observed on ZnO (*55, 56*), as well as with bands observed on complex zinc hydrides, supposed to be bridged (Table 3). These bands can be observed only if the pretreatment temperature is sufficiently high. They are almost nonexistent if pretreatment is carried out at 673 or 723 K. The stronger pretreatment used in the present work, compared with our previous work (*28*), frees new sites as a result of the enhanced dehydroxylation of the surface (Fig. 5). There are also ν(OH) and ν(OD) bands on ZnCr oxide after hydrogen and deuterium adsorption, respectively. However, their position and relative intensity do not differ significantly from those of the normal hydroxy and deuteroxy groups arising from water dissociation.

When hydrogen and deuterium are brought into contact with the activated CoCr oxide, a very sharp, strong band is formed at 1660 and 1200 cm^{-1}, respectively, certainly due to terminal M–H and M–D stretches (Fig. 6). Another weaker band is observed at 1762 and 1276 cm^{-1}, respectively, also assigned to similar species (Table 2). Very weak bands are also probably present near 1700 and 1685 cm^{-1} after H_2 adsorption.

On the low-frequency side of the main sharp band another much broader absorption is always present near 1605 cm^{-1}, better evident in subtraction spectra (Fig. 6). The position and shape of this band would be in line with an assignment to the deformation mode of adsorbed water. However, when deuterium is adsorbed a similar band is observed near 1160 cm^{-1}. The isotopic shift agrees with that forecast for a metal hydride species more than for adsorbed water [scissoring modes of gaseous H_2O and D_2O 1595 and 1178 cm^{-1} (*29*), respectively, with a ratio of 1.35]. We therefore assign these bands to bridged metal–hydride and –deuteride stretches, according to their shape. The samples of CoCr are rather opaque in the ν(OH) region, preventing detailed analysis of the bands. However, when deuterium is adsorbed a band grows at 2694 cm^{-1}, with a shoulder at 2700 cm^{-1}. These are typical ν(OD) frequencies of free deuteroxy groups on both chromia and metal chromites.

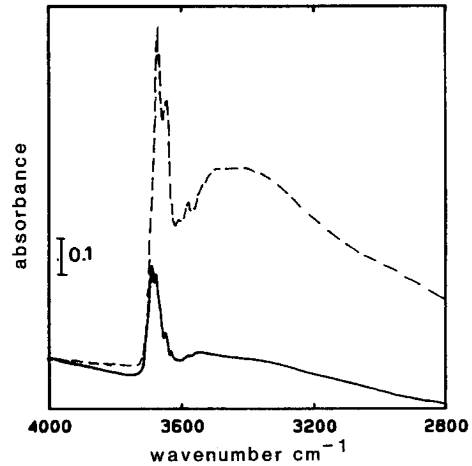

FIG. 5. FT-IR spectra of ZnCr oxide [ν(OH) region] activated in hydrogen/vacuum at 673 K (broken line) and 793 K (solid line).

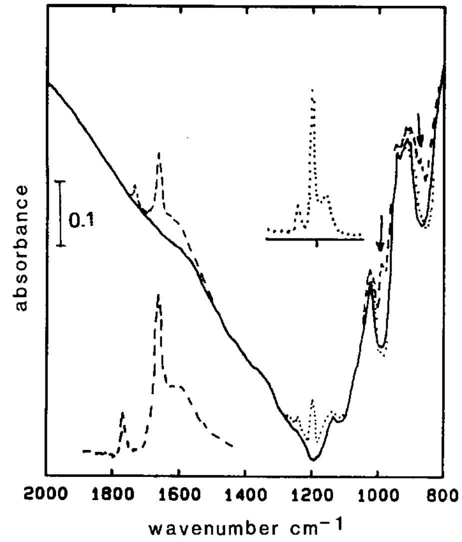

FIG. 6. FT-IR spectra of CoCr oxide after activation (solid line) and after contact with hydrogen (120 Torr; broken line) and deuterium (120 Torr; dotted line). In the insets the corresponding subtraction spectra are reported. Arrows refer to two bands cited in the text.

When the MnCr oxide is exposed to hydrogen and deuterium, weak sharp bands appear at 1506 and 1090 cm^{-1}, respectively (Fig. 7). Broader bands at 1240 and near 900 cm^{-1} are also observed in the two cases, respectively. According to the band frequency and shape, assignments can be given to terminal and bridged hydride and deuteride species, as reported in Table 2. When hydrogen and deuterium are adsorbed ν(OH) (3720 cm^{-1}, shoulder, 3695 cm^{-1}, 3655 cm^{-1}) and ν(OD) (2745 cm^{-1}, shoulder, 2725 and 2690 cm^{-1}) bands also grow. They correspond to the bands formed by water and heavy water dissociative adsorption.

The assignment to metal–hydrogen stretches of the bands cited so far is in agreement with the frequencies reported in the literature for these modes in chromium, zinc, cobalt, and manganese hydrides, some of which are summarized in Table 3. After all hydrogen adsorption experiments we have also tried to find deformation modes of metal hydride bonds in the region below 1000 cm^{-1}. However, this region is perturbed by the slight shifts or intensity modifications of multiphonon bands, as already reported by Scarano *et al.* for CO adsorption on chromia (*19*). This makes it very difficult to use subtraction spectra in searching for weak bands in this region. In the case of the ZnCr oxide both hydrogen and deuterium adsorption cause the disappearance of a sharp band at 837 cm^{-1} and the appearance of a new sharp one at 968 cm^{-1} (Fig. 4). As already mentioned, the lack of a detectable isotopic shift would indicate that the latter band is due to a vibration that does not involve hydrogen primarily.

With the CoCr oxide, hydrogen adsorption causes the formation of bands at 990 and 875 cm^{-1} (Fig. 6). These absorptions do not appear after deuterium adsorption and, consequently, are thought to be due to vibrational modes of surface hydrogen species. The band at 990 cm^{-1} can be tentatively assigned to the asymmetric metal–hydrogen–metal stretch of bridged hydride species or to another type of species such as triply bridged hydrides; cf. the more intense ν(Co–H) band detected at 958 cm^{-1} for the complex [Co(Cp)H]$_4$ (*45*). The band at 875 cm^{-1} could be due to a Co–H deformation mode; this assignment agrees with

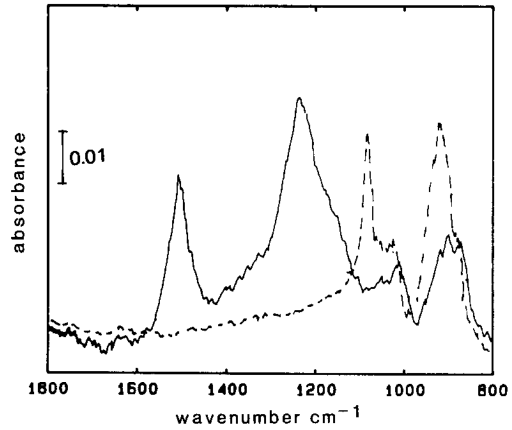

FIG. 7. FT-IR spectra of the adsorbed species arising from contact of activated MnCr oxide with hydrogen (120 Torr; solid line) and deuterium (120 Torr; broken line).

the values of the deformation frequency observed on $[HCo(CO)_4]$—(ν(CoH) 1934 cm^{-1}, δ(CoH) 704 cm^{-1} (*42*)—and $[HCo(CN)_5]^{3-}$—ν(CoH) 1840 cm^{-1}, δ(CoH) 774 cm^{-1} (*44*)—and with the general observation that the lower the stretching frequency the higher the deformation. Neither on chromia nor on MnCr oxide were we able to identify other bands involving adsorbed hydrogen.

DISCUSSION

The adsorption of hydrogen on chromia has been the object of a number of studies. The most recent studies concluded that hydrogen can dissociate producing chromium hydrides (*6, 7*), identified as active species in hydrogenation. Our data provide confirmation of the formation of terminal chromium hydride species at room temperature on reduced chromia. The weakness of the bands observed can be due either to the small extinction coefficient of these absorptions or to the small number of active sites for dissociative adsorption, as concluded by Burwell and co-workers (*6*).

The spectra of the surface species arising from hydrogen adsorption on the three chromites have several common features. In all cases relatively sharp bands, certainly split in the case of the ZnCr and CoCr oxides, but possibly also in the case of the MnCr oxide, are observed at higher frequencies, together with broader bands at lower frequencies. From the data we report in Table 3, it is very reasonable to assign the sharp bands in all cases to terminal hydride species on oxidized cations. It is worth mentioning that hydrogen on cobalt metal is reported to produce ν(CoH) bands at relevantly higher frequencies [1840 cm^{-1} on Co/Al_2O_3 (*51*) and 2030 cm^{-1} for Co^0–H species on CoO–MgO solid solutions (*52*)]. A possible assignment of the bands to chromium hydrides is unproposable in the cases of ZnCr and MnCr, but seems unlikely also for the main bands observed on CoCr, although the ν(CrH) and ν(CoH) frequencies may fall in the same region. It is possible that the two extremely weak bands at 1700 and 1685 cm^{-1} are due to CrH in this case. The relative trend of the frequencies $\nu(ZnH) > \nu(CoH) > \nu(MnH)$ for these terminal species on the chromites agrees with that of metal–hydride homogeneous complexes having similar coordination spheres, and suggests that the terminal hydrides formed on the three chromites involve the three cations probably in the bivalent state and in similar environments.

Our results compare well with data for the related hydride species formed on the surfaces of ZnO–MgO and CoO–MgO solid solutions, reported recently. The frequencies observed on these surfaces [1786, 1707, and 1663 cm^{-1} for ν(ZnH) (*53*) and 1669, 1585, and 1542 cm^{-1} for ν(CoH) (*52*)] are not far from those we observed on zinc and cobalt chromites. The authors of these papers have assigned the ν(ZnH) band at 1780 cm^{-1} and the ν(CoH) band at 1669 cm^{-1} to hydride species on isolated M^{2+} cations on the edges of crystals of the MgO matrix. On these edges the cations would be in an incomplete coordination with respect to the octahedral coordination of the bulk. According to electronic absorption data these authors then assign these species to cations in distorted tetrahedral coordination. On the other hand, on ZnO (where Zn^{2+} ions have tetrahedral coordination) hydrogen adsorption forms terminal species characterized by a main band at 1711 cm^{-1} (*54, 55*) with a smaller one at higher frequency, 1750 cm^{-1} (*56*). On the basis of the known normal spinel structure of the zinc, cobalt, and manganese chromites (*20*) it seems reasonable to assign the main band we observe in each case to hydride species on M^{2+} ions in an incomplete tetrahedral coordination.

The detection of a doublet of bands due to terminal hydrides with the higher-frequency component having weaker intensity is common to CoCr and ZnCr. It is tempting to relate this splitting to the very likely presence of a fraction of Zn^{2+} and Co^{2+} ions in octahedral positions, according to the cation distribution forecast in solid solution spinels (*16, 57, 58*). A higher ν(M–H) frequency could be expected for cations in higher coordination.

With our ZnCr, CoCr, and MnCr oxides broader bands at lower frequencies are also observed, assigned to bridged hydride species. As already mentioned, two stretching modes (asymmetric and symmetric) are observed in the case of bridged metal–hydride complexes, whose frequency difference grows as a function of the metal–hydrogen–metal angle (*34*). The broad bands we observe in the region 1700–1200 cm^{-1} must then be due to the asymmetric stretching mode, which is expected to shift up more the larger is the bond angle. The trend we observe for these bands is ν(CoHCo) > ν(ZnHZn) > ν(MnHMn) and this might be rationalized on the basis of geometric factors. In fact, although the lattice parameters of the three stoichiometric chromite spinels follows the order Mn > Co > Zn (*20*), by enhancing the excess of bivalent cations the lattice parameters of both ZnCr and CoCr are modified. The measured value of the lattice parameter of the calcined ZnCr material is distinctly higher than that of calcined CoCr (a = 0.836 nm for ZnCr and 0.828 nm for CoCr). Smaller cation–cation distances could justify stronger interactions M···H···M and, consequently, higher angles and higher ν_{as}(MHM) frequencies. The assumption that these species bridge between two bivalent cations is tentative and is based only on the similarity between the band we observe on ZnCr and that reported on ZnO.

As already noted, in almost all cases we observe, in addition to the formation of ν(MH(D)) bands, the growth of ν(OH(D)) bands. This could be seen as consistent with heterolytic dissociative adsorption of hydrogen, $H_2 + M^{2+}O^{2-} = M^{2+}H^- + OH^-$. However, in all the present cases, these bands are superimposed on those of normal hydroxy or deuteroxy groups, free from hydrogen bonding. This behavior is different from that observed upon hydrogen dissociation on oxides such as ZnO (*54–56*) and MgO (*59*), where the appearance of ν(MH) bands parallels that of "special" ν(OH) bands, generally at relatively low frequency and rather broad. In our case we cannot be sure that the ν(OH) and ν(OD) bands formed during hydrogen and deuterium adsorption are due to the heterolytic dissociation of hydrogen. It is not excluded that, in our cases, the ν(OH) and ν(OD) bands grow as a result of a reductive adsorption phenomenon, $H_2 + 2\,O^{2-} = 2\,OH^- + 2e^-$, and by isotopic exchange, $OH^- + D_2 = OD^- + HD$. A similar conclusion was also drawn in relation to the detection of hydride species by hydrogen dissociation on ThO_2 (*60*) and ZrO_2 (*61*). In both cases, homolytic dissociation has been hypothesized.

The classical heterolytic dissociative adsorption of hydrogen has been related to the basicity of the surface oxide ions (*52, 59, 62*), which would represent the driving force necessary to break heterolytically the H_2 molecule. However, a number of hydrogenation catalysts are not typically basic materials, but are simple or complex oxides of transition metals or rare earths. In particular, chromia and chromites, used for decades as hydrogenation catalysts, do not seem to be extremely basic. What chromites probably have in common with chromia, ZnO, ZrO_2, and ThO_2 (all of which are oxides active in hydrogenations and which produce hydride species upon hydrogen adsorption), besides a certain basicity, is the possibility of slight reduction, with the appearance of n-type semiconducting character when working under reducing conditions. Many years ago Garcia de la Banda (*63*) and other workers reported the relationship of the catalytic activity and hydrogen absorption capacity to the electronic conductivity of both chromia and zinc chromites. It is not excluded that forms of hydrogen dissociation other than the heterolytic one, such as dissociative ionosorption by reaction of hydrogen with nearly free electrons, are active on these catalysts, with the consequent production of the hydride species we observe.

It may be noted that the hydrogen adsorption mechanism is apparently similar on the three nonstoichiometric spinel catalysts studied here, although their catalytic behavior in CO hydrogenation is remarkably different. ZnCr and MnCr are selective catalysts for the production of alcohols from syngas, while CoCr behaves as a methanation and Fischer–Tropsch catalyst. This may be related to the fact that only on CoCr catalyst are reduced centers observed on which bridged and even triply bridged carbonyls are formed from CO adsorption. On the other oxides only terminal carbonyls on oxidized cations are found. According to general opinion (*64*), the different behavior of the cobalt compound can be related to the tendency of bridged carbonyls to dissociate. This would result in methane and hydrocarbon formation.

ACKNOWLEDGMENTS

The author is indebted to Degussa A. G. (Hanau, West Germany) for kindly supplying a noncommercial chromia sample, to Professors A. Vaccari and F. Trifirò (University of Bologna, Bologna, Italy) for the preparation of cobalt and zinc chromite catalysts, and to Professor P. Forzatti and his co-workers (Politecnico di Milano, Milan, Italy) for the preparation of the manganese chromite catalyst. This work has been supported by the Italian Government, Ministero della Pubblica Istruzione (fondi 40%).

REFERENCES

1. Burwell, R. L., Haller, G. L., Taylor, K. C., and Read, J. F., *Adv. Catal.* **20,** 1 (1969).
2. Khodakov, Y. S., Makarov, P. A., Delzer, G., and Minachev, Kh. M., *J. Catal.* **61,** 184 (1980).
3. Natta, G., *in* "Catalysis" (P. H. Emmett, Ed.), Vol. 3, p. 349. Reinhold, New York, 1955.
4. Tronconi, E., Cristiani, C., Ferlazzo, N., Forzatti, P., Villa, P. L., and Pasquon, I., *Appl. Catal.* **32,** 285 (1987).
5. Wagner, F. S., *in* "Applied Industrial Catalysis" (B. E. Leach, Ed.), Vol. 2, p. 29. Academic Press, New York, 1983.
6. Ely, S. R., and Burwell, R. L., *J. Colloid Interface Sci.* **65,** 244 (1978).
7. Engelhardt, J., and Valyon, J., *in* "Hydrogen Effects in Catalysis" (Z. Paál, and P. G. Menon, Eds.), p. 565. Dekker, New York, 1988.
8. Adkins, H., and Connor, R., *J. Amer. Chem. Soc.* **53,** 1091 (1931); Jalowiecki, L., Wrobel, G., Daage, M., and Bonnelle, J. P., *J. Catal.* **107,** 375 (1987).
9. Molstad, M. C., and Dodge, B. F., *Ind. Eng. Chem.* **27,** 134 (1935); Riva, A., Trifirò, F., Vaccari, A., Busca, G., Mintchev, L., Sanfilippo, D., and Manzatti, W., *J. Chem. Soc. Faraday Trans. 1* **83,** 2213 (1987).
10. Frohlich, P. K., and Cryder, D. S., *Ind. Eng. Chem.* **22,** 1051 (1930); Forzatti, P., Cristiani, C., Ferlazzo, N., Lietti, L., Pasquon, I., Tronconi, E., Villa, P. L., Antonelli, G. B., Sanfilippo, D., and Contarini, S., *in* "Proceedings, IX Simposio Ibero-americano de Catalisis, Guanajuato, Maxico, 1988," Vol. 2, p. 671.
11. Stiles, A. B., *in* "Applied Industrial Catalysis" (B. E. Leach, Ed.), Vol. 2, p. 110. Academic Press, New York, 1983.
12. Fornasari, G., Gusi, S., Trifirò, F., and Vaccari, A., *Ind. Eng. Chem. Res.* **26,** 1500 (1987).
13. Giamello, E., Fubini, B., Bertoldi, M., Busca, G., and Vaccari, A., *J. Chem. Soc. Faraday Trans. 1* **85,** 237 (1989).
14. Busca, G., and Vaccari, A., *J. Chem. Soc. Chem. Commun.*, 788 (1988).
15. Del Piero, G., Di Conca, M., Trifirò, F., and Vaccari, A., *in* "Reactivity of Solids" (P. Barret, and L. C. Dufour, Eds.), p. 1029. Elsevier, Amsterdam, 1985.
16. Trifirò, F., Vaccari, A., and Busca, G., to be published.
17. Bellotto, M., Cristiani, C., Ferlazzo, N., and Forzatti, P., to be published.
18. Zecchina, A., Coluccia, S., Guglielminotti, E., and Ghiotti, G., *J. Phys. Chem.* **75,** 2774 (1971).
19. Scarano, D., Zecchina, A., and Reller, A., *Surface Sci.* **198,** 11 (1988).
20. Cormack, A. N., Lewis, G. V., Parker, S. C., and Catlow, C. R. A., *J. Phys. Chem. Solids* **49,** 53 (1988).
21. Sheppard, N., and Nguyen, T. T., *in* "Advances in Infrared and Raman Spectroscopy" (R. J. H. Clark, and R. E. Hester, Eds.), Vol. 5, p. 67. Heyden, London, 1978.
22. Baltanas, M. A., Stiles, A. B., and Katzer, J. R., *J. Catal.* **88,** 516 (1984).
23. Harrison, P. G., and Thornton, E. W., *J. Chem. Soc. Faraday Trans. 1* **74,** 2703 (1978).
24. Mohana Rao, K., Spoto, G., Guglielminotti, E., and Zecchina, A., *J. Chem. Soc. Faraday Trans. 1* **84,** 2195 (1988).
25. Ansorge, J., and Förster, H., *J. Catal.* **68,** 182 (1981).
26. Mohana Rao, K., Scarano, D., Spoto, G., and Zecchina, A., *Surface Sci.* **204,** 319 (1988).
27. Marshall, R., Mitra, S. S., Gielisse, P. J., Plendl, J. N., and Mansur, L. C., *J. Chem. Phys.* **43,** 2893 (1965).

28. Busca, G., and Vaccari, A., *J. Catal.* **108,** 491 (1987).

29. Nakamoto, K., "Infrared and Raman Spectra of Inorganic and Coordination Compounds," 4th ed. Wiley, New York, 1986.

30. Van Zee, R. J., DeVore, T. C., and Weltner, W., *J. Chem. Phys.* **71,** 2051 (1979).

31. Jordan, R. F., and Norton, J. R., *J. Amer. Chem. Soc.* **104,** 1255 (1982).

32. Thaler, E., Folting, K., Huffmann, J. C., and Caulton, K. G., *Inorg. Chem.* **26,** 374 (1987).

33. Girolami, G. S., Salt, J. E., Wilkinson, G., Thornton-Patt, M., and Hursthouse, M. B., *J. Amer. Chem. Soc.* **105,** 5954 (1983).

34. Howard, M. W., Jayasooriya, V. A., Kettle, S. F. A., Powell, D. B., and Sheppard, N., *J. Chem. Soc. Chem. Commun.,* 18 (1979).

35. Herzberg, G., "Spectra of Diatomic Molecules." Van Nostrand, Princeton, 1950.

36. Kubas, G. J., and Shriver, D. F., *Inorg. Chem.* **9,** 1951 (1970).

37. Billups, W. E., Konarski, M. M., Hauge, R. H., and Margrave, J. L., *J. Amer. Chem. Soc.* **102,** 7393 (1980).

38. Chang, S. C., Hauge, R. H., Kafafi, Z. H., Margrave, J. L., and Billups, W. E., *J. Chem. Soc. Chem. Commun.,* 1682 (1987).

39. Kubas, G. J., and Shriver, D. F., *J. Amer. Chem. Soc.* **92,** 1949 (1970).

40. Ashby, E. C., and Watkins, J. J., *Inorg. Chem.* **16,** 1445 (1977).

41. Kruse, W., and Atalla, R. H., *J. Chem. Soc. Chem. Commun.,* 921 (1968).

42. Edgell, W. F., and Summitt, R., *J. Amer. Chem. Soc.* **83,** 1772 (1961).

43. Bressan, M., and Rigo, P., *Inorg. Chem.* **17,** 769 (1978).

44. Banks, R. G. S., and Pratt, J. M., *J. Chem. Soc. A,* 854 (1968).

45. Andrews, J. A., Jayasooriya, U. A., Oxton, I. A., Powell, D. B., Sheppard, N., Jackson, D. F., Johnson, B. F. G., and Lewis, J., *Inorg. Chem.* **19,** 1035 (1980).

46. Van Zee, R. J., DeVore, T. C., Wilkerson, J. R., and Weltner, W., *J. Chem. Phys.* **69,** 1869 (1978).

47. Miles, W. J., and Clark, R. J., *Inorg. Chem.* **7,** 1801 (1977).

48. Davison, A., and Faller, J. W., *Inorg. Chem.* **6,** 845 (1967).

49. Howard, M. W., Skinner, P., Bhardwaj, R. K., Jayasooriya, V. A., Powell, D. B., and Sheppard, N., *Inorg. Chem.* **25,** 2846 (1986).

50. Kaesz, H. D., Fellmann, W., Wilkes, G. R., and Dahl, L. F., *J. Amer. Chem. Soc.* **87,** 2753 (1965).

51. Kavtaradze, N. K., and Sokolova, N. P., *Russ. J. Phys. Chem.* **44,** 1485 (1970).

52. Zecchina, A., and Spoto, G., *Z. Phys. Chem.* **137,** 173 (1983).

53. Ghiotti, G., and Boccuzzi, F., *J. Chem. Soc. Faraday Trans. 1* **79,** 1843 (1983).

54. Eischens, R. P., Pliskin, W. A., and Low, M. J. D., *J. Catal.* **1,** 180 (1962).

55. Boccuzzi, F., Borello, E., Zecchina, A., Bossi, A., and Camia, M., *J. Catal.* **51,** 150 (1978).

56. Saussey, J., Rais, T., and Lavalley, J. C., *Bull. Soc. Chim. Fr.,* 305 (1985).

57. Del Piero, G., Trifirò, F., and Vaccari, A., *J. Chem. Soc. Chem. Commun.,* 656 (1984).

58. Escard, J., Mantin, I., and Sibut-Pinote, R., *Bull. Soc. Chim. Fr.,* 3403 (1970).

59. Coluccia, S., Boccuzzi, F., Ghiotti, G., and Morterra, C., *J. Chem. Soc. Faraday Trans. 1* **78,** 2111 (1982).

60. Lamotte, J., Lavalley, J. C., Lorenzelli, V., and Freund, E., *J. Chem. Soc. Faraday Trans. 1* **81,** 215 (1985).

61. Kondo, J., Abe, H., Sakata, Y., Maruya, K., Domen, K., and Onishi, T., *J. Chem. Soc. Faraday Trans. 1* **84,** 511 (1988).

62. Tanabe, K., *in* "Catalysis by Acids and Bases" (B. Imelik *et al.,* Eds.), p. 1. Elsevier, Amsterdam, 1985.

63. Garcia de la Banda, J. F., *J. Catal.* **1,** 136 (1962); Garcia de la Banda, J. F., *in* "Electronic Phenomena in Adsorption and Catalysis on Semiconductors" (K. Hauffe, and Th. Wolkenstein, Eds.), p. 83. de Gruyter, Berlin, 1969.

64. van der Lee, G., and Ponec, V., *Catal. Rev. Sci. Eng.* **29,** 183 (1987).